Journal of the Optical Society of Korea, Vol. 6, No. 2, June 2002, pp. 21-26

Measurement of Highly Aspherical Surface using Computer Generated Holograms

Tae-hee Kim* and Soon Cheol Choi

Digital Media R&D Center,
SAMSUNG ELECTRONICS CO., Kyungki-Do 442-742, KOREA

(Received December 07, 2001)

Interferometric metrology with a null CGH(computer-generated hologram) is presented for measuring highly aspheric surfaces used in a large screen projection television system with high accuracy. The cubic spline surface model which works in a single-pass configuration with a refractive index of object space 0 is used for designing a null CGH. A hybrid null corrector with plano-concave lens in front of a CGH is presented to make the CGH easier to fabricate. Experimental results are presented to demonstrate the validity of the proposed technique.

OCIS codes : 090.1760, 120.3180, 220.4840

I. INTRODUCTION

Lenses used in large screen projection television system a have become progressively more aspheric and difficult to test, while at the same they have been required to give better images. Surface errors in these lenses are measured directly using interferometers with null correctors, which compensate for the aspheric departure of the surface [1,2]. The application of a CGH as null corrector allows aspherical surfaces to be measured easily without using expensive null lenses [3]- [5].

The CGH design usually uses the standard phase fitting model of specifying CGH functions as a power series with even terms. But, the CGH is poorly modeled using a power series with a reasonable number of terms because the phase function on the CGH required for testing highly aspheric optics has a cusp at the center. In the cubic spline phase surface model, the CGH can be directly constructed by algebra and trigonometry based on an exact geometrical model [4].

The size of the ring spacing must not become too small because the cost and difficulty of the CGH fabrication will go up. In the grating equation, the ring spacing depends on the angle of the incident ray, so an incident ray with fast slope repuires small for ring spacing. This means a concave lens can be put in front of the CGH to increase the ring spacing.

In this paper, a CGH design using a cubic spline surface model is presented to solve some problems in using the standard phase fitting model. A null corrector consisting of a plano-concave lens and CGH operating in tandem with a Fizeau interferometer to test an convex aspherical surface is presented to make the CGH easier to fabricate. The experimental results are presented to demonstrate the validity of the proposed technique.

II. DESIGN OF NULL CGH

1. Cubic spline phase surface model

A circular hologram which has several advantages for testing axisymmeteric optics is used. The phase distribution on the CGH is derived using an exact analytic model of the rays normal to the surface under test. The parameters for this derivation are shown in Fig. 1.

The CGH design is simplified by treating it in single-pass which assume the refractive index of object space as 0 to easily find a normals to the surface under test. The CGH for testing the surface is used at the image point I. These equations lead to the optical path length (OPL) from the object point O′ on the surface under test to image point I

$$\mathrm{OPL} = \mathrm{O'H'} + \mathrm{H'I} \tag{1}$$

The OPL variation across the CGH is OPD(optical path difference). Choosing the arbitrary reference point as the center, the OPD across the CGH

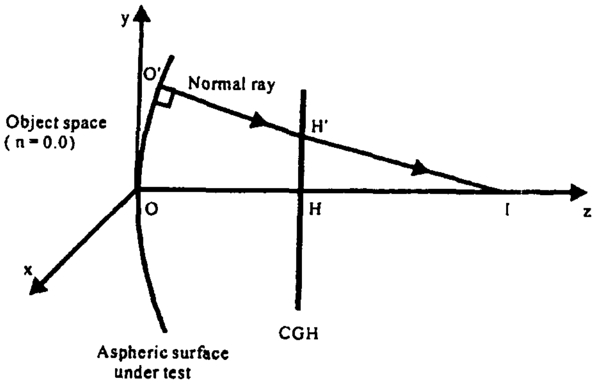

FIG. 1. Geometry for defining a CGH such that it returns the same wavefront as a perfect aspheric surface.

$$\mathrm{OPD} = \mathrm{OPL} - (\mathrm{OH} + \mathrm{HI}) \tag{2}$$

The standard phase fitting model adds phase to the radial position on the CGH according to the following polynomial expansion:

$$\mathrm{OPD} = M\sum_{i=1}^{N} A_i \rho^{2i} \tag{3}$$

$$\rho = \sqrt{x^2 + y^2}$$

The trigonometry and algebra provide the following relations:

$$\mathrm{O'H'} = \sqrt{(\mathrm{O'_x} - \mathrm{H'_x})^2 + (\mathrm{O'_y} - \mathrm{H'_y})^2 + (\mathrm{O'_z} - \mathrm{H'_z})^2} \tag{4}$$

$$\mathrm{H'I'} = \sqrt{(\mathrm{H'_x} - \mathrm{I'_x})^2 + (\mathrm{H'_y} - \mathrm{I'_y})^2 + (\mathrm{H'_z} - \mathrm{I'_z})^2} \tag{5}$$

$$\mathrm{OH} = \mathrm{H_z} - \mathrm{O_z} \tag{6}$$

$$\mathrm{HI} = \mathrm{I_z} - \mathrm{H_z} \tag{7}$$

where M is the operating diffraction order, N is the number of polynomial coefficients in the series, A_i is the coefficient on the $2i$-th power of ρ, which is the normalized radial aperture coordinate. In this model, the OPD is obtained by optimizing the polynomial coefficients using data at values $\rho = 0, ..., 1$.

Fig. 2 shows the lens under test. 71 mm f/0.30 aspheric concave surface deviates from the best-fit surface by 1000 μm and 88 mm f/4.1 aspheric convex surface deviates from the best-fit surface by 1600 μm.

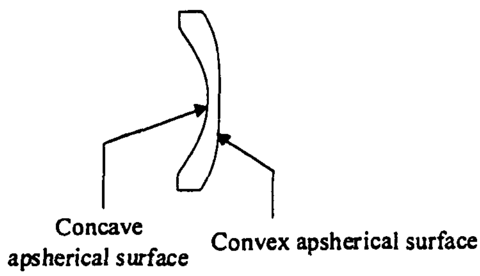

FIG. 2. Layout of lens under test

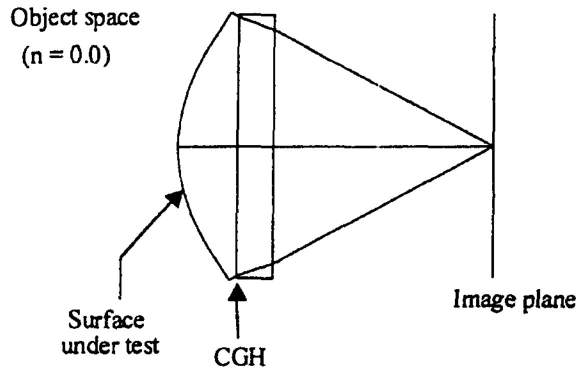

FIG. 3. Optical configuration for designing the CGH which tests a concave apsherical surface.

Fig. 3 shows the configuration for designing the null CGH for a concave aspheric surface. We first designed the null CGH using the standard phase fitting model, Eq. (7), using over 80 phase coefficients. The wavefront residual at an image plane is shown in Fig. 4(a). The peak-to-valley residual error at the image plane is almost 20 waves at 633 nm. It can be seen that the standard phase fitting model can't properly describe the OPD on the CGH because the final quality of the tested surface depends on errors introduced at the image plane by a null CGH.

A cubic spline phase surface model can properly describe the CGH with accurate OPD data. For this example, 1000 position points along the the radial direction on the CGH are picked off and then OPDs at 1000 positions from Eq. (6) are directly calculated. With given data points (OPD_1,ρ_1), ... (OPD_{1000}, ρ_{1000}), a cubic interpolating spline for these points is constructed.

The peak-to-valley wavefront residual at a image plane, as shown in Fig. 4(b), has been reduced less than 0.01 waves at the 633 nm test wavelength. This represents an improvement of over four orders of magnitude over the null CGH designed with the standard

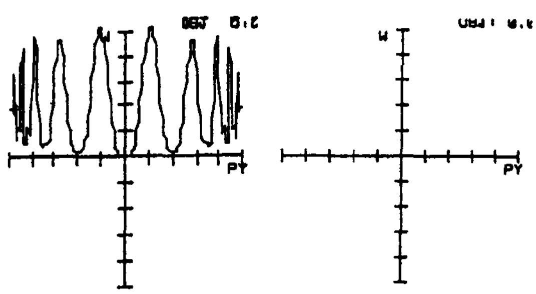

(a) (b)

FIG. 4. (a) Wavefront residual using standard phase fitting model. (b) Wavefront residual using cubic spline phase surface model.

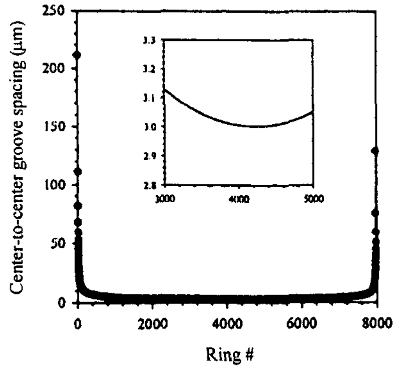

FIG. 5. Center-to-center groove spacing for CGH used in first order to test a concave aspherical surface. Hologram contains 7972 rings in diameter of 35 mm.

phase fitting model.

The CGH is encoded by specifying a phase function for the diffraction to create. For use in the M-th order, the CGH will consist of one plotted fringe for every M waves in the phase function. Fig. 5 shows the center-to-center groove spacing calculated for CGH used in first order. The largest center-to-center groove spacing is 2361.81 μm at the center and the smallest center-to-center groove spacing is 3.00 μm in the middle of the hologram.

2. Hybrid null corrector

Fig. 6(a) shows the configuration for designing the null CGH for a convex aspheric surface. The CGH is designed using a cubic spline model based on rays normal to the spherical mirror which is used to retroreflect the light transmitted through the test lens.

Fig. 7(a). shows the center-to-center groove spacing of the designed CGH for using in first order. The largest center-to-center groove spacing is 2361.81 μm at the center and the smallest center-to-center groove spacing is 1.00 μm in the middle of the hologram.

In the grating equation, the ring spacing depends on the angle of the incident ray, so the incident ray

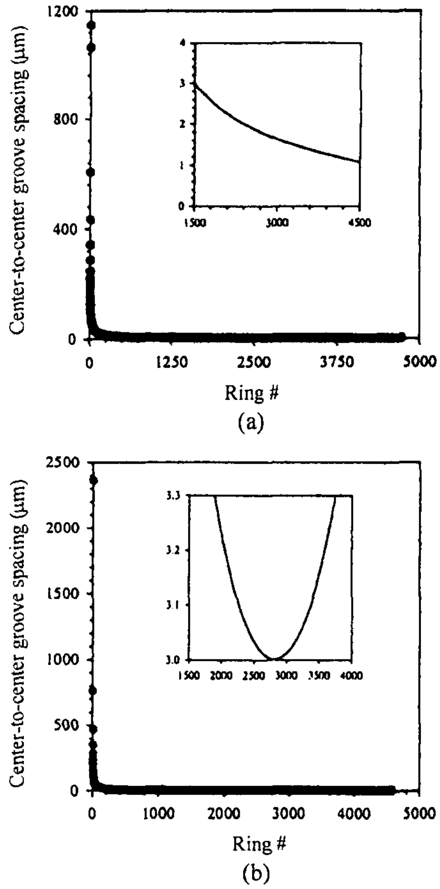

FIG. 6. Center-to-center groove spacing for CGH used in first order to test a convex aspherical surface. (a) Without plano-concave lens (b) with plano-concave lens in front of CGH. In the case of (b), hologram contains 4237 rings in diameter of 28.5 mm.

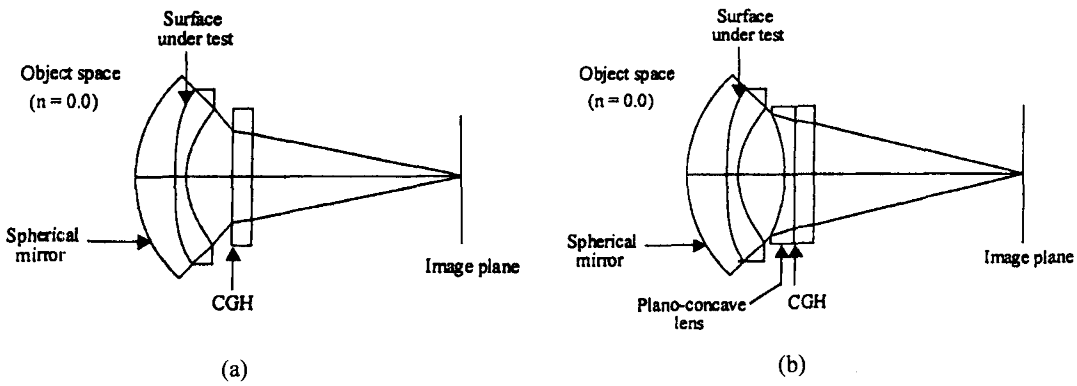

FIG. 7. Optical configuration for designing the CGH which tests a convex apsherical surface. (a) Without plano-concave lens (b) with plano-concave lens in front of CGH.

TABLE 1. Null CGH structure parameters

Parameters	Values (at 632.8 nm)	
	CGH for convex	CGH for concave
Grating type	Binary phase grating	
Material (glass)	Fused silica ($n_{\text{glass}} = 1.46$)	
Operating mode	Transmission	
Diffraction order	1-st order	
Averaging grating spacing	6.73 μm	4.38 μm
Grating groove depth	1λ (2π radian)	
Grating duty-cycle	50%	

with fast slope requires small ring spacing. The concave lens which decreases the slope of the incident ray is useful for correcting the spacing between adjacent rings on the hologram.

Fig. 6(b) shows the layout of the optical system in which the plano-concave lens is located in front of the CGH for designing a CGH for testing the convex surface. Fig. 7(b) shows the ring spacing of CGH after applying the plano-concave lens to the system. The reasonable improvement that the ring spacing of 1 μm is increased to 3 μm, making the part easier to fabricate, can be seen.

Table 1 summarizes the stated parameters for the Null CGH. The CGH is designed to be used in the +1 diffraction order transmission mode. The hologram has a glass substrate with an index of refraction of n = 1.46. It has a grating groove depth of π radians and a 50% duty-cycle. The CGH is fabricated using a circular laser writing system [6].

III. MEASUREMENT SYSTEM ASSEMBLY

The apsherical surfaces are tested by phase-shifting Fizeau interferometer (Wyko-6000) with a diverging lens (ZYGO, F# 0.75) and CCD (736 by 480 pixels). The test lens is illuminated with a He-Ne laser (λ = 632.8 nm). The experimental setup for testing a concave asphere is shown in Fig. 8(a). The incident light transmits through CGH and strikes the concave asphere at normal incidence for all points. This transmitted beam is retro-reflected by the asphere surface to form the test wavefront. The experimental setup for a testing convex asphere is shown in Fig 8(b). The incident light transmits through both of CGH and test lens and strikes the spherical mirror at normal incidence for all points. This transmitted beam is retro-reflected by the spherical mirror to form the test wavefront. In the Figs. 8(a) and 8(b), the spatial filter is used to block unwanted orders of diffraction. For correctly aligning the components, the CGH, plano-concave lens and test lens have 5-axis (tip/tilt, x, y, z-axis) adjustment, respectively.

IV. RESULTS

Wavefront tilt and power terms are removed from the raw phase map in order to reduce alignment errors during the interferometric measurements. Then the data are low pass filtered to reduce high frequency noise. The processed interferogram, 2-D, and 3-D phase maps of the concave surface are shown in Figs. 9 (a), (b), and (c). The surface under test has the rms figure error of 1.4 waves and peak-to-valley surface figure error of 7.3 waves. The non-axisymmetric errors in Fig. 9 were measured independently using the rotation test with the concave surface. Since the

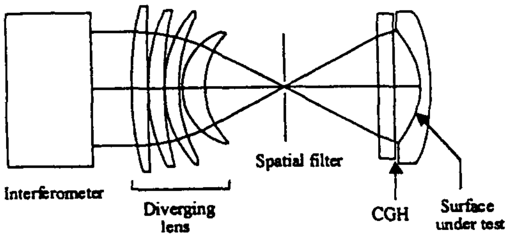

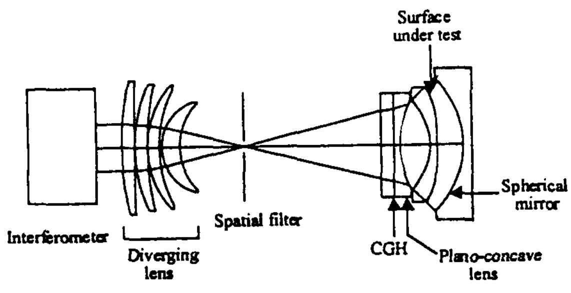

FIG. 8. (a) Experimental setup for testing concave asphere (b) Experimental setup for testing convex asphere

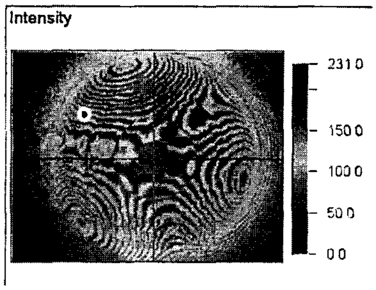

(a)

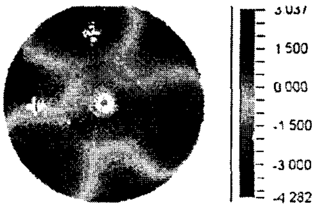

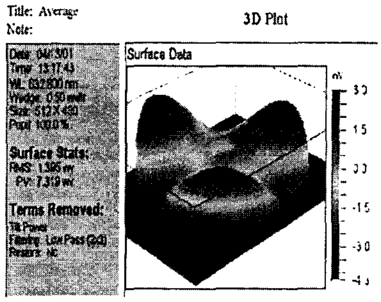

(b) (c)

FIG. 9. (a) Interferogram, (b)2-D phase map, and (c) 3-D phase map of concave aspherical surface acquired through the null CGH with Fizeau interferometer.

errors rotated with lens from three independent measurements, the non-axisymmetric errors were confirmed to be in the concave asphere.

Figs. 10 (a) and (b) show the interferogram and 2-D phase map after removing tilt, power, and high frequency noise from transmission wavefront obtained by convex surface measurement system. The inverse of fiducial mark between the phase maps of Fig. 9(b) and Fig. 10(b) is due to reflection by spherical mirror.

The transmission wavefront can be expressed as

$$\mathrm{TRW} = -2S_1(n-1) - 2S_2(n-1) + 2S_3 \qquad (8)$$

where S_1, S_2, and S_3 are figure errors of concave surface, convex surface, and spherical mirror, respectively. n is the refractive index of the test lens. Figure error of S_3 become negligible in Eq. (8) since the error is small as 0.03 wave rms. Solving Eq. (8) for S_2, the convex surface error is given by

$$S_2 = \frac{1}{2(n-1)}[2S_1(n-1) - \mathrm{TRW}] \qquad (9)$$

For mapping these phases in subtracting the transmission wavefront from the concave surface error, two fiducial marks were put on the concave surface and interferometer was keeping the same zoom position during measuring process.

Figs. 11(a) and (b) shows 2-D and 3-D phase map obtained from Eq. (9). It can be seen that the convex surface under test has the rms figure error of 2.9 waves

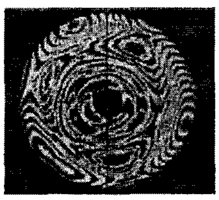

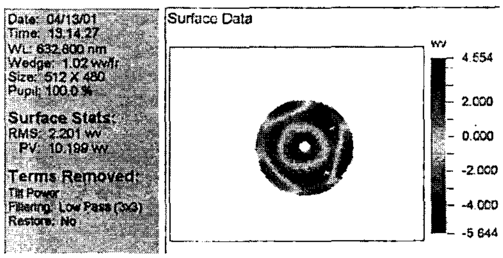

(a) (b)

FIG. 10. (a) Interferogram and (b) 2-D phase map of transmission wavefront acquired through the hybrid null corrector (plano-concave lens and CGH) with Fizeau interferometer.

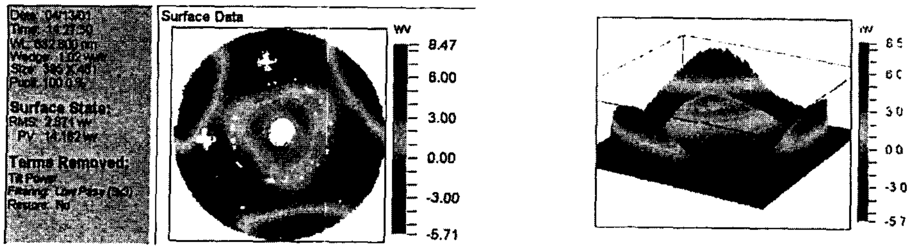

(a) (b)

FIG. 11. (a) 2-D phase map and (b) 3-D phase map of convex surface acquired from subtracting transmission wavefront from concave surface error.

and peak-to-valley surface figure error of 14.2 waves.

V. CONCLUSIONS

The phase CGHs for testing highly aspherical surfaces are designed to be used in the 1-st order transmission mode. These are designed for all rays to coincide with the normals of aspherical surface after diffraction. We describe that the null CGH with a total of 1000 OPDs as spline points. This work in the cubic spline phase surface model with the single-pass configuration in which the refractive index of object space is 0. We find that the concave lens is useful for correcting the spacing between adjacent rings on the hologram. Applying the concave lens to the system in which ring spacing decreases with increasing ring radius, we can get the reasonable improvement that the ring spacing of 1 μm is increased to 3 μm, making the part easier to fabricate. The data obtained by the constructed measurement system suggest an rms accuracy of measurement of 1 waves and an rms repeatability of 0.2 waves.

*Corresponding author : thkim3@samsung.co.kr.

REFERENCES

[1] Jose M. Sasian, Opt. Eng. **27**, 1051 (1988).
[2] Scott A. Lerner, Jose M. Sasian, Opt. Eng. **39**, 1796 (2000).
[3] Yu-Chun Chang, "Diffraction wavefront analysis of computer-generated holograms", Ph. D. dissertation (Optical Sciences Center, University of Arizona, 1999).
[4] James H. Burge, "Advanced techniques for measuring primary mirrors for astronomical telescopes", Ph. D. dissertation (Optical Sciences Center, University of Arizona, 1993).
[5] J.H.Burge, Proc. SPIE **2871**, 362 (1997).
[6] Institute of Automation and Electrometry, Laboratory of Laser Technologies, Novosibirsk, Russia, 2000.